Ultracold Collision Properties of Metastable Alkaline-Earth Atoms

Andrei Derevianko and Sergey G. Porsev*
Department of Physics, University of Nevada, Reno, Nevada 89557

Svetlana Kotochigova, Eite Tiesinga, and Paul S. Julienne
Atomic Physics Division, National Institute of Standards and Technology, 100 Bureau Drive, Stop 8423, Gaithersburg, Maryland 20899

(Received 21 October 2002; published 13 February 2003)

Ultracold collisions of spin-polarized ^{24}Mg, ^{40}Ca, and ^{88}Sr in the metastable $^3P_2$ excited state are investigated based on molecular potentials obtained from *ab initio* calculations. We calculate the long-range interaction potentials and estimate the scattering length and the collisional loss rate as a function of magnetic field. The scattering lengths show resonance behavior due to the appearance of a molecular bound state in a purely long-range interaction potential and are positive for magnetic fields below 50 mT. A loss-rate model shows that losses should be smallest near zero magnetic field and for fields slightly larger than the resonance field, where the scattering length is also positive.

DOI: 10.1103/PhysRevLett.90.063002 PACS numbers: 32.10.Dk, 33.55.Be, 34.10.+x, 39.25.+k

Exploring ultracold collision physics with metastable $(nsnp)\,^3P_2$ alkaline-earth atoms [1–5] promises insights that complement those obtained from the more conventional atomic species used in laser cooling. Unlike alkali-metal atoms [6,7] the most common alkaline-earth atoms have no nuclear spin, which greatly simplifies a theoretical description [8]. Furthermore, in contrast to metastable noble-gas collisions [9] the low electronic energy of the alkaline-earth metastable states ensures the absence of collisionally induced Penning or associative ionization.

Atomic collisions in the ultracold regime play a crucial role on the road toward quantum degenerate gases. We show here that polarized metastable $(nsnp)\,^3P_2$ alkaline-earth systems with projection $m = 2$ along the magnetic field might satisfy the key requirements for this quest: a positive scattering length and a favorable ratio of elastic to inelastic collision rates for certain magnetic field strengths. In addition, we show how a new type of pure long-range molecular states can allow the resonant magnetic field control of the scattering length. These states arise due to an interplay of an anisotropic (quadrupole) interaction and the magnetic field. Similar anisotropy has been predicted to exist for polar molecule collisions in an electric field [10]. Many-body systems with anistropic interactions might now be explored [11].

Trapping of metastable alkaline earths in magneto-optical [2–5] and magnetic traps [2–4,12] has been demonstrated. A $\sim$1 s magnetic trap lifetime for densities near 10^{10} atoms/cm^3 is observed with metastable ^{88}Sr in experiments at Rice and Tokyo Universities [3,13]. These trap lifetimes are limited by background collisions rather than by the radiative lifetime, which is on the order of minutes [1].

Molecular potentials.—We have calculated short-range adiabatic potentials correlating to two $^3P_2$ atoms using a molecular *ab initio* relativistic valence-bond method, as previously described [14]. A variety of attractive and repulsive potentials, and a number of short-range avoided crossings appear among them. Strong collisional loss processes are likely [8] if the atoms approach one another on the attractive curves. The section below shows how a magnetic field can be used to manipulate long-range properties in such a way as to create pure long-range molecular states and prevent some of these losses.

Atomic structure calculations and Rayleigh-Schrödinger perturbation theory allow us to express the long-range adiabatic potentials in terms of multipole moments of the atoms [15]. The matrix elements of the Hamiltonian for two $^3P_2$ atoms up to order $1/R^6$, where R is the internuclear separation, are [16]

$$\langle x|H_{lr}|y\rangle = \frac{\langle x|V_{QQ}|y\rangle}{R^5} + \sum_{j,j'=1}^{3} \langle x|A_{jj'}|y\rangle \frac{C_6^{jj'}}{R^6}\,. \qquad (1)$$

Here $|x\rangle$ and $|y\rangle$ are product states $|^3P_2, \Omega_1\rangle|^3P_2, \Omega_2\rangle$, Ω_α is the projection of the total electron angular momentum $j_\alpha = 2$ of atom α on the internuclear axis. Also $\Omega = \Omega_1 + \Omega_2$ is a good quantum number in the Hund's case (c) coupling scheme. The two terms on the right hand side of Eq. (1) describe the quadrupole-quadrupole (QQ) and the second-order dipole-dipole (DD) interaction.

Matrix elements of the QQ interaction are expressed in terms of the quadrupole moment $\mathcal{Q}$ of the $^3P_2$ state [1]. For this paper the value of $\mathcal{Q}$ is recalculated using a more accurate many-body technique [17]. The values are 8.46(8) $E_h a_0^5$, 12.9(4) $E_h a_0^5$, and 15.6(5) $E_h a_0^5$ for metastable Mg, Ca, and Sr, respectively. Here E_h is a Hartree, 1 a_0 is 0.0529 nm, and one-standard deviation uncertainties, based on convergence studies of the many-body theory, are given in parenthesis. The $C_6^{jj'}$ are intermediate dipole-dipole dispersion coefficients, calculated following Ref. [18], and tabulated in Table I. The $\langle x|A_{jj'}|y\rangle$

TABLE I. Intermediate dispersion coefficients $C_6^{jj'}$ in units of $10^3\ E_h a_0^6$. The C_6 are symmetric in j and j' and have a 10% one-standard deviation uncertainty.

	C_6^{11}	C_6^{21}	C_6^{22}	C_6^{31}	C_6^{32}	C_6^{33}
Mg*	3.19	−3.70	4.40	6.47	−7.60	13.2
Ca*	7.74	−10.4	14.1	19.0	−25.8	50.6
Sr*	13.3	−17.1	22.3	35.0	−46.8	109

only depend on angular momentum algebra and are given in Ref. [16].

The Hund's case (c) adiabatic potentials that connect to our short-range valence-bond calculation are obtained by diagonalizing Eq. (1) within the $|^3P_2, \Omega_1\rangle|^3P_2, \Omega_2\rangle$ basis. (See, for example, Ref. [1].).

Magnetic field.—A magnetic field **B** modifies the long-range interaction of two metastable alkaline-earth atoms profoundly. For each atom α the approximate Zeeman Hamiltonian $H_{Z\alpha} = \mu_B(\mathbf{j}_\alpha + \mathbf{s}_\alpha)\cdot\mathbf{B}$ has been added to the other terms in the molecular Hamiltonian. Here, $\mathbf{s}_\alpha$ is the electron spin of atom α, μ_B is the Bohr magneton, and we have assumed that the atomic gyromagnetic ratio of the electron orbital angular momentum and spin are 1 and 2, respectively. The magnetic field lifts the degeneracy with respect to the projection m_α of $\mathbf{j}_\alpha$ along the space-fixed magnetic field direction. Forces due to the interatomic interaction break this space-fixed quantization, and align the molecular angular momentum along the internuclear axis. This results in loss of polarization of the angular momentum.

The long-range adiabatic molecular potentials in the presence of a magnetic field are found by diagonalizing $H_{Z1} + H_{Z2} + H_{lr}$ within the $^3P_2 + {}^3P_2$ product basis. These potentials $U(R, \theta_B)$ not only depend on the field strength but also on the angle θ_B between the internuclear axis and **B**. Figure 1 shows all Sr_2 gerade adiabatic potentials for a 10 mT field and $\theta_B = 45°$. The nine dissociation limits are separated by about $E/k_B = 10$ mK and are labeled by $M = m_1 + m_2$, where $M = +4(-4)$ for the highest (lowest) dissociation limit. k_B is the Boltzmann constant.

Figure 1 shows a multitude of avoided crossings for internuclear separations where the Zeeman splitting is comparable to the quadrupole-quadrupole interactions, that is, avoided crossings appear for $R \approx R_B \equiv \sqrt[5]{Q^2/(\mu_B B)}$. For Sr* and $B = 10$ mT, R_B is $\sim 100 a_0$. For $R < R_B$ the QQ interactions dominate and the Hund's case (c) $\Omega_g^{\pm}$ molecular potentials correlating to two $^3P_2$ atoms are recovered.

Experiments trap the "low-field seeking" spin-polarized $m_\alpha = +2$ state [3,4]. The topmost potential in Fig. 1 dissociates to this limit. The radial and angular dependence of this potential $U_{m_1=2,m_2=2}(R, \theta_B)$ is shown in Fig. 2. Four long-range hills and valleys are visible for $R > R_B$ and a repulsive hard core that is nearly independent of angle appears for $R \approx R_B$.

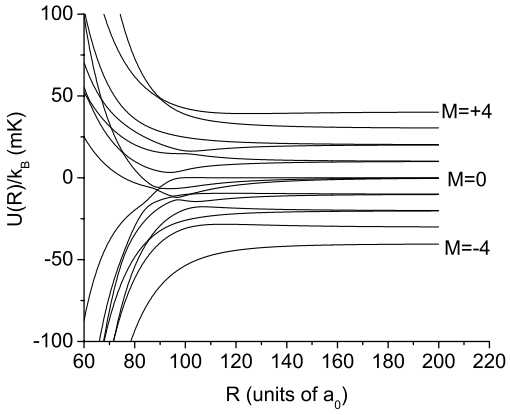

FIG. 1. Long-range gerade adiabatic potentials correlating to two $^3P_2$ Sr atoms for $B = 10$ mT and $\theta_B = 45°$.

The behavior of $U_{2,2}(R, \theta_B)$ is further illuminated when it is expanded in terms of Legendre polynomials $P_L(x)$,

$$U_{2,2}(R, \theta_B) = \sum_{L=0,2,4,\ldots} U_L(R)\, P_L(x), \qquad (2)$$

where $x = \cos\theta_B$. The $U_L(R)$ of Sr_2 are shown in Fig. 3. For $R \gg R_B$, U_4 is largest and is dominated by the QQ interaction. In Fig. 2 it gives rise to the hills and valleys. For $R \approx R_B$, contributions of other components are appreciable, while for $R \lesssim 60\, a_0$ the repulsive $U_0(R)$ dominates. The inset of Fig. 3 shows that $U_0(R)$ has a shallow attractive region for large R, that becomes deeper and wider for increasing B. This so-called "Zeeman–van der Waals" well is a consequence of an interplay between Zeeman and anisotropic quadrupole-quadrupole interactions.

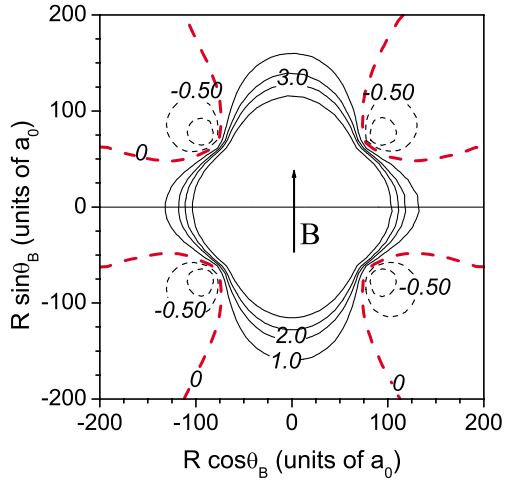

FIG. 2 (color online). Polar plot of the adiabatic potential for two spin polarized Sr* atoms at $B = 10$ mT. Equipotential curves are shown as dashed, thick dashed, and solid contours for energies that are lower than, equal to, and higher than the dissociation energy of the two atoms, respectively. The contour values are given in mK. The arrow indicates the direction of **B**.

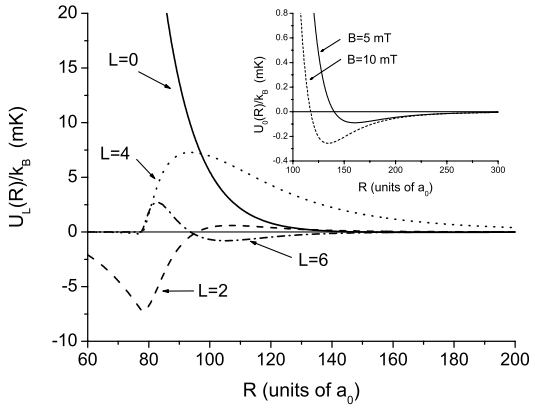

FIG. 3. The coefficients $U_L(R)$ of Eq. (2) for Sr_2 as a function of internuclear separation and $B = 10$ mT. The inset shows $U_0(R)$ for $B = 5$ and 10 mT.

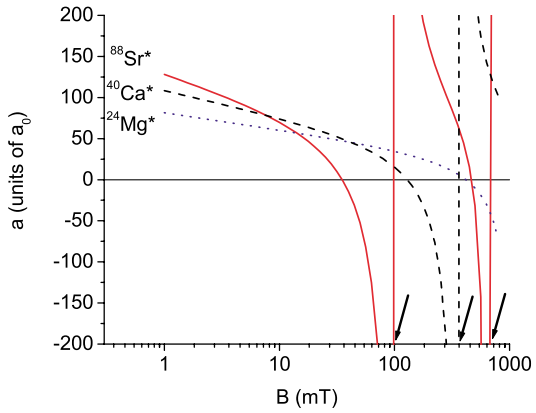

FIG. 4 (color online). Scattering length of the $U_0(R)$ potential of spin polarized $^3P_2$ atoms as a function of magnetic field. Values for ^{24}Mg, ^{40}Ca, and ^{88}Sr are shown. The arrows show the magnetic fields for which zero-energy resonances occur.

For $R \gg R_B$, an analytical expression for $U_{2,2}$ can be derived based on perturbation theory around $|^3P_2, m_1\rangle|^3P_2, m_2\rangle$ with the quantization axis along **B**. We find for the contribution of the QQ interaction

$$U_{2,2}^{(QQ)} = \frac{3}{2}\frac{Q^2}{R^5} P_4(x), \tag{3}$$

and for the DD interaction

$$U_{2,2}^{(DD)} = -\frac{1}{R^6}[C_6^{(0)} + C_6^{(2)} P_2(x) + C_6^{(4)} P_4(x)]. \tag{4}$$

The monopole coefficient $C_6^{(0)}$ is independent of B and is 1000 $E_h a_0^6$, 3300 $E_h a_0^6$, and 6200 $E_h a_0^6$ for Mg*, Ca*, and Sr*, respectively. Consequently, the long-range behavior of $U_0(R)$ is given by an attractive $1/R^6$ potential that is independent of B.

Scattering lengths.—A rigorous description of elastic collisions between spin-polarized metastable $^3P_2$, $m = 2$ atoms should start from $B = 0$ theories [19] and extend those to include the Zeeman interaction [7]. Such a model is beyond the scope of this paper. Instead, we take advantage of our understanding of the adiabatic potentials in a magnetic field. Nuclear motion couples the electronic potentials via so-called nonadiabatic couplings. These couplings are strongest near avoided crossings between adiabatic electronic potentials and lead to inelastic losses. For example, a transition from the $M = 4$ to $M = 3$ curves in Fig. 1 results in depolarization and conversion of internal energy to kinetic energy.

First we will assume that adiabaticity holds. We relax this assumption below. The zero-energy s-wave ($l = 0$) scattering length of polarized metastable $^3P_2$ $m = 2$ atoms is then given by the scattering length of the $U_0(R)$ component of $U_{2,2}(R, \theta_B)$. This length for three alkaline-earth species as a function of magnetic field is shown in Fig. 4. For $B < 40$ mT the scattering lengths are large and positive and a Bose condensate would be stable against collapse. Uncertainties in QQ and DD coefficients do not change the picture significantly.

For $B > 70$ mT the scattering lengths exhibit singularities, where a is infinite. These resonances are due the appearance of the first bound state in $U_0(R)$. The inset of Fig. 3 shows that for increasing B the well becomes wider and deeper, supporting an increasingly larger number of bound states and thus extra resonances.

Magnetic field control of the sign and magnitude of the scattering length near the resonances appears likely for these systems. Magnetic field-induced resonance behavior in scattering lengths has been observed for alkali-metal atoms. There, however, the singularity is a consequence of Feshbach resonances rather than through the appearance of extra bound states in an adiabatic potential.

Inelastic processes.—The scattering lengths have been determined assuming that nonadiabatic couplings and losses are negligible. We verify the applicability of the adiabatic approximation by estimating loss rates from a two-channel curve-crossing model. The model has an attractive van der Waals potential in an incoming channel, $|i\rangle$, of two spin-polarized atoms and $l = 0$ that crosses a repulsive C_5/R^5 exit channel, $|e\rangle$, of two atoms with $m_1 + m_2 < 4$ and $l = 4$. The coupling, C_5'/R^5, is due to the QQ interaction. More precisely,

$$V_{2\mathrm{ch}} = \begin{pmatrix} -C_6^{(0)}/R^6 & C_5'/R^5 \\ C_5'/R^5 & C_5/R^5 + 20\hbar^2/2\mu R^2 - \Delta \end{pmatrix}, \tag{5}$$

where μ is the reduced mass of the dimer, $\Delta \propto B$ is the difference in dissociation energy of the two states, the exit state has a $l = 4$ centrifugal potential, and $C_6^{(0)}$ is defined in Eq. (4). The two states cross near R_B.

The R-dependent eigenvalues of $V_{2\mathrm{ch}}$ are our model adiabatic potentials. In fact, the topmost adiabat plays the role of the $L = 0$ component of the U_{22} adiabat. It has an attractive van der Waals tail and a repulsive wall

that is to be compared to the "Zeeman–van der Waals" well of Fig. 3.

Loss can occur when the atoms reach short-range R on the incoming channel or when the atoms are reflected into the repulsive exit channel. We numerically solved the two coupled Schrödinger equations assuming a hard wall placed inside R_B and parameter values valid for strontium. This approach has no losses due to short-range inelastic processes. Nevertheless, we feel that the model gives an order of magnitude estimate of the loss rate. The calculations show that for B from 1 to 5 mT the loss rate K into the exit channel rapidly rises from $\sim 10^{-13}$ cm^3/s to 10^{-11} cm^3/s due to Wigner threshold effects in the exit channel. For large fields the rate decreases slowly and exponentially with B and for $B \approx 500$ mT has dropped to 10^{-12} cm^3/s.

The loss rate and the scattering length show a resonance similar to the resonances shown in Fig. 4 when an extra bound state appears in the upper adiabat. For collision energies below 1 μK the loss rate approaches zero in a narrow ≈ 1 mT region above the resonance location where the scattering length is large and positive. For collision energies above 100 μK the resonance is broadened and will be hard to observe. The position of the resonance and the corresponding loss rate will change when all coupled channels are included. However, the resonance and a (partial) drop in the loss rate is expected to survive.

Consequently, we have identified magnetic field regions where losses for strontium are smaller than or on the order of 10^{-13} cm^3/s, i.e., for $B < 1$ mT and for magnetic field strengths just above the resonance. For several Tesla fields the loss rate will be small as well. At a rate constant of 10^{-13} cm^3/s the imaginary part of the scattering length $hK/(2\mu)$ [20] is orders of magnitude smaller than the real part of the scattering length shown in Fig. 4. The collision is adiabatic for these field regions and the scattering length is meaningful. Moreover, these rates lead to sample lifetimes of 1 s at densities of 10^{13} cm^{-3}.

Conclusion.—We have calculated the interaction potentials of metastable alkaline-earth dimers in the presence of a magnetic field. A purely long-range interaction potential is found to determine the scattering length between two spin-polarized $^3P_2$ alkaline-earth atoms. A magnetic-field-induced resonance is observed, where the interaction potential supports an extra bound state. Reference [10] predicts similar long-range states for polar molecules in an electric field. The existence of such molecular states should be a general property of colliding atoms or molecules with an anisotropic interaction potential in an external field that split a degeneracy.

Although full-scale multichannel calculations of magnetic trap losses and scattering lengths are desirable, a two-channel model indicates that the inelastic loss rate of the collision between two spin-polarized atoms are small for small magnetic field strengths and above the field-induced resonance, where the scattering length is positive. We uncovered several unique features of collisions between metastable alkaline earths, which may offer new insights into the physics of utlracold quantum gasses.

This work was supported in part by the National Science Foundation and the office of Naval Research. The work of S. G. P. was supported in part by the Russian Foundation for Basic Research under Grant No 02-02-16837-a.

*Permanentt address: Petersburg Nuclear Physics Institute, Gatchina, Leningrad district, 188300, Russia.

[1] A. Derevianko, Phys. Rev. Lett. **87**, 023002 (2001).
[2] H. Katori, T. Ido, Y. Isoya, and M. Kuwata-Gonokami, in *Atomic Physics 17: Proceedings of the 17th International Conference, ICAP 2000, Florence, Italy* (AIP, New York, 2001).
[3] S. B. Nagel *et al.*, Phys. Rev. A **67**, 011401(R) (2003).
[4] T. Loftus *et al.*, in Proceedings of the International Conference on Atomic Physics, Boston, 2002.
[5] J. Grünert and A. Hemmerich, Phys. Rev. A **65**, 041401 (2002).
[6] K. Burnett *et al.*, Nature (London) **416**, 21 (2002).
[7] E. G. M. van Kempen, S. J. J. M. F. Kokkelmans, D. J. Heinzen, and B. J. Verhaar, Phys. Rev. Lett. **88**, 093201 (2002); F. H. Mies, E. Tiesinga, and P. S. Julienne, Phys. Rev. A **61**, 022721 (2000); J. P. Burke, Jr, J. L. Bohn, B. D. Esry, and C. H. Greene, Phys. Rev. A **55**, 2511 (1997).
[8] M. Machholm, P. Julienne, and K.-A. Suominen, Phys. Rev. A **64**, 033425 (2001).
[9] A. Robert *et al.*, Science **292**, 461 (2001); F. P. Dos Santos *et al.*, Phys. Rev. Lett. **86**, 3459 (2001); M. R. Doery *et al.*, Phys. Rev. A **58**, 3673 (1998).
[10] A. V. Avdeenkov and J. L. Bohn, Phys. Rev. Lett. **90**, 043006 (2003).
[11] S. Yi and L. You, Phys. Rev. A **66**, 013607 (2002).
[12] T. Loftus, J. R. Bochinski, and T. W. Mossberg, Phys. Rev. A **65**, 013411 (2002).
[13] H. Katori (private communication).
[14] E. Tiesinga, S. Kotochigova, and P. Julienne, Phys. Rev. A **65**, 013403 (2002).
[15] A. Dalgarno and W. D. Davison, in *Advances in Atomic Molecular Physics*, edited by D. Bates and I. Estermann (Academic Press, New York, 1966), Vol. 2, p. 1.
[16] A. Derevianko and A. Dalgarno, Phys. Rev. A **62**, 062501 (2000).
[17] S. Porsev, M. Kozlov, Y. G. Rakhlina, and A. Derevianko, Phys. Rev. A **64**, 012508 (2001).
[18] S. G. Porsev and A. Derevianko, Phys. Rev. A **65**, 020701 (2002).
[19] F. H. Mies, Phys. Rev. A **7**, 942 (1973); B. Zygelman, A. Dalgarno, and R. D. Sharma, Phys. Rev. A **49**, 2587 (1994); B. Gao, Phys. Rev. A **54**, 2022 (1996).
[20] N. Balakrishnan, R. Forrey, and A. Dalgarno, Chem. Phys. Lett. **280**, 1 (1997).